Mon. Not. R. Astron. Soc. **373,** 1245–1250 (2006) doi:10.1111/j.1365-2966.2006.11122.x

Chaotic zone boundary for low free eccentricity particles near an eccentric planet

Alice C. Quillen⋆ and Peter Faber⋆

Department of Physics and Astronomy, University of Rochester, Rochester, NY 14627, USA

Accepted 2006 September 26. Received 2006 September 22; in original form 2006 August 2

ABSTRACT

We consider particles with low free or proper eccentricity that are orbiting near planets on eccentric orbits. Through collisionless particle integration, we numerically find the location of the boundary of the chaotic zone in the planet's corotation region. We find that the distance in semimajor axis between the planet and boundary depends on the planet mass to the 2/7 power and is independent of the planet eccentricity, at least for planet eccentricities below 0.3. Our integrations reveal a similarity between the dynamics of particles at zero eccentricity near a planet in a circular orbit and with zero free eccentricity particles near an eccentric planet. The 2/7th law has been previously explained by estimating the semimajor at which the first-order mean motion resonances are large enough to overlap. Orbital dynamics near an eccentric planet could differ due to first-order corotation resonances that have strength proportional to the planet's eccentricity. However, we find that the corotation resonance width at low free eccentricity is small; also the first-order resonance width at zero free eccentricity is the same as that for a zero-eccentricity particle near a planet in a circular orbit. This accounts for insensitivity of the chaotic zone width to planet eccentricity. Particles at zero free eccentricity near an eccentric planet have similar dynamics to those at zero eccentricity near a planet in a circular orbit.

Key words: celestial mechanics – planetary systems : protoplanetary discs.

1 INTRODUCTION

Chaotic diffusion associated with the overlap of resonances has been shown to be responsible for instabilities in the Solar system (e.g. see Lecar, Franklin & Murison 1992; Holman & Wisdom 1993; Lecar et al. 2001; Tsiganis et al. 2005). For the restricted three-body problem, Wisdom (1980) first showed that the width of the chaotic zone near a planet could be explained by calculating the location at which the first-order mean motion resonances are large enough to overlap. The zone width has been measured numerically and predicted theoretically (Wisdom 1980; Duncan, Quinn & Tremaine 1989; Murray & Holman 1997) for a planet in a circular orbit, though some work has extended the stability analysis for bodies in orbits near circular and eccentric binary stars (Holman & Wiegert 1999; Mudryk & Wu 2006). The stability of bodies at low eccentricity, residing in multiple planet extrasolar systems has also been investigated numerically (e.g. Rasio & Ford 1996; Barnes & Raymond 2004; Lepage & Duncan 2004).

Recently, Quillen (2006b) suggested that the edge of Fomalhaut's eccentric ring could be due to truncation by a 0.1 eccentricity Neptune mass planet. The nearby star, Fomalhaut, hosts a ring of circumstellar material (Aumann 1985; Gillett 1985) residing between 120 and 160 au from the star (Holland et al. 1998; Dent et al. 2000; Holland et al. 2003). *Spitzer Space Telescope* infrared observations of Fomalhaut reveal a strong brightness asymmetry in the ring (Stapelfeldt et al. 2004; Marsh et al. 2005). Recent *Hubble Space Telescope* (*HST*) observations show that this ring has both a steep and an eccentric inner edge (Kalas, Graham & Clampin 2005). The sharp disc edge suggested that the dust particles are in orbits with low free or proper eccentricity; thus, the ring has eccentricity equal to the forced eccentricity caused by secular perturbations from the proposed planet. Such a configuration is possible if inelastic collisions in the disc damp the eccentricities of particles, resulting in a particle distribution that moves along nearly closed streamlines or closed and non-self-intersecting orbits. Fomalhaut's ring has a intermediate collision time-scale of 10^3 orbits, estimated from its normal disc opacity $\tau \sim 1.6$ m at 24 m (Marsh et al. 2005).

While previous theoretical and numerical studies have considered orbit stability near the corotation region for planets on circular orbits, little work has been done considering the stability of orbits near a planet on an eccentric orbit. The dynamical problem of an object orbiting a planet in a circular orbit has a conserved quantity, the Jacobi integral, that is not conserved when the planet is on an eccentric orbit. Surfaces of section have been used to illustrate the types of orbits (tori or area filling) for the restricted three-body system (Wisdom 1985; Winter & Murray 1997). However, when

⋆E-mail: aquillen@pas.rochester.edu (ACQ); pfaber@mail.rochester.edu (PF)

the planet is eccentric, there is no extra integral of motion making it difficult to create surfaces of section. We are motivated here to consider the role of the planet's eccentricity in setting the boundary of non-stochastic orbits in the corotation region. We focus here on particle orbits that have nearly zero free eccentricity and so have eccentricity set by the forced eccentricity due to secular perturbations from the planet.

2 NUMERICAL INTEGRATIONS

Numerical integrations were carried out in the plane, using massless and collisionless particles under the gravitational influence of only the star and a massive planet with eccentricity, $e_{\rm p}$, using a conventional Burlisch–Stoer numerical scheme. A particle near a planet on an eccentric orbit feels secular perturbations from the planet if it is located away from low-order mean motion resonances. The particle's eccentricity and longitude of periastron precess about a point set by the distance to the planet, the planet's eccentricity longitude of periastron. The secular motion can be described in terms of a free (or proper) and forced eccentricity (e.g. Murray & Dermott 1999). Only a particle with zero free eccentricity would have a fixed argument of periastron and eccentricity. In our integrations, the initial particle eccentricities were set to the predicted forced eccentricity due to secular perturbations from the planet and the longitudes of periastron were chosen to be identical to that of the planet. Initial mean anomalies were randomly chosen. Particles were removed from the integration when their eccentricity was larger than $e_{\rm max} = 0.9$. We work in units of the planet's semimajor axis, $a_{\rm p}$, and orbital period. The mass of the planet is described in terms of its mass ratio, μ, the ratio of the mass of the planet to that of the central star.

2.1 Measurement of the width of the chaotic zone

As a function of an initial semimajor axis, we measured the lifetimes of particles before removal from the integration. The semimajor axis bins for each lifetime measurement had width d$a = 0.01$, and 100 particles were integrated for each bin. An abrupt increase in the particle lifetime was seen in the simulations as a function of initial semimajor axis (see fig. 2 by Quillen 2006b). Inside the chaotic zone, particles were scattered to high eccentricity and removed from the simulation, but outside it, the lifetime of particles exceeded 10^4 orbits. For planet mass ratios between 10^{-3} and 10^{-5} and eccentricities between 0.05 and 0.2, we measured the semimajor axis, a_z, at which this transition in lifetime occurred. The distance d$a = (a_z - a_{\rm p})/a_{\rm p}$ between this semimajor axis and that of the planet, divided by the planet's semimajor axis, is plotted in Fig. 1.

In Fig. 1, we note that the chaotic zone boundaries depend on the planet mass. The scaling is consistent with that predicted from the 2/7th law or

$$ {\rm d}a = 1.5\mu^{2/7} \qquad (1) $$

(Wisdom 1980), where the constant 1.5 is taken from numerical measurements by Duncan et al. (1989). The offset between the line predicted by equation (1) is not significant as we have measured the width from an ensemble of particles and required them all to remain at least for 10^4 orbits. This implies that we have measured a location outside the last stable orbit in a surface section or a closed orbit radius versus energy bifurcation plot. The points shown in Fig. 1 include those integrated for a zero-eccentricity planet, so the offset between that predicted by the 2/7th law is the same for the higher planet eccentricities as for the zero planet eccentricity. Using finer spacing in semimajor axis and by restricting the initial orbital elements rather than choosing them randomly, it is possible to find stable orbits somewhat closer to the planet. The offset from the predicted line is caused by the measurement procedure, rather than the planet eccentricity. We note an increased scatter in the chaotic zone boundary at lower masses in Fig. 1; however, we find no clear trend in the scatter as a function of planet eccentricity. Since the particle lifetimes in the chaotic zone are longer for the lower-mass planets, more particle trajectories may need to be integrated to achieve the same precision in the measurement of the chaotic zone boundary at lower planet masses. The choice of initial random mean anomalies could also contribute to the scatter at lower planet masses.

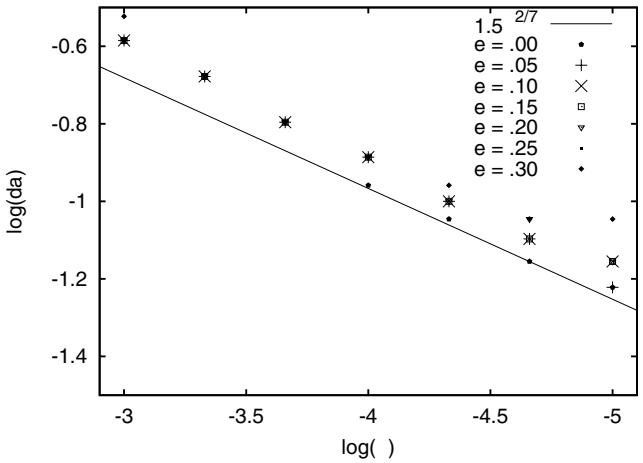

Figure 1. The distance between the planet semimajor axis and that of the chaotic zone boundary is plotted as a function of planet mass ratio, μ. Points are plotted at the semimajor axis at which particles' lifetime exceeded 10^4 orbits. Each point type corresponds to a different planet eccentricity. The points lie on top of one another because the chaotic zone width is independent of the planet eccentricity for orbits with zero free eccentricity. Particles were initially placed in orbits with zero free eccentricity and arguments of periastron the same as that of the planet. The solid line corresponds to that predicted by equation (1).

Fig. 1 shows points corresponding to integrations with different planet eccentricities. The points for integrations near eccentric planets lie on top of those at low or zero planet eccentricity. In other words, the width of the chaotic zone appears to be independent of the planet eccentricity. We find that there exists a long-lived low free eccentricity region near moderately eccentric planets (in the planar problem). This region has d $a < e_{\rm p}$ for the more highly eccentric planets and so is nearer to the planet's major axis than to the planet's periastron. In other words, these orbits pass closer to the star than to the periastron of the planet, but since they are apsidally aligned with the orbit of the planet they do not cross the planet's orbit.

A disc with a low collision rate, could evolve to a distribution with nearly closed orbits fixed about the forced eccentricity and apsidally aligned with a planet. Our planar numerical integrations show that this region is stable over long time-scales (greater than 10^4 orbits) and so could host a long-lived planetesimal distribution.

2.2 Dispersion and lifetimes

We have also measured the eccentricity distribution after 10^4 planetary orbits in the disc edge. These are shown in Fig. 2. Each point shown in this figure corresponds to measurements based on integration of 100 particles. The corotation chaotic region arises from

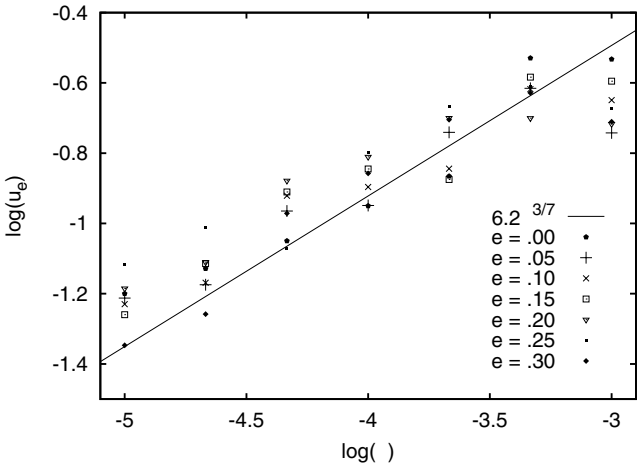

Figure 2. Eccentricity dispersion, u_e, in the disc edge as a function of planet mass. The line shown is $u_e = 6.2\mu^{3/7}$ and consistent with that predicted with equation (19) for particles near a planet in a circular orbit. Each point type corresponds to integrations containing a planet with a different eccentricity. The eccentricity dispersion is not strongly dependent on the planet eccentricity.

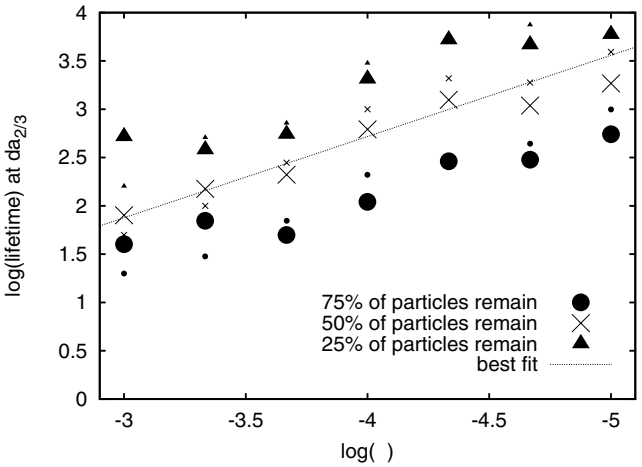

Figure 3. Particle lifetime in planetary orbits as a function of planet mass for particles with initial semimajor axis two-third of the way between the planet's semimajor axis and the chaotic zone boundary. The large and small points are for planet eccentricities $e_p = 0.05$ and 0.2, respectively. The circles, crosses and triangles correspond to times when 75, 50 and 25 per cent of the particles remain in the simulation, respectively. The line shown has lifetime equal to 0.23 $\mu^{-0.84}$. Particles have initial angle of pericentre identical to that of the planet and zero free eccentricity. The lifetimes are not strongly dependent on the planet eccentricity.

resonance overlap. However, outside the chaotic zone mean motion resonances exist that affect the particles, but since they do not overlap other mean motion resonances the particles do not vary their orbital parameters stochastically or do vary stochastically but on much longer time-scales. Fig. 2 shows that the velocity dispersion in the stable boundary is likely to depend on planet mass and not on eccentricity.

To characterize the lifetime of particles in the chaotic zone, we consider particles within initial semimajor axis at two-third the distance in semimajor axis to the zone edge. The time-scale for removal of 25, 50 and 75 per cent of the particles is plotted as a function of planet mass for planet eccentricities, $e_p = 0.05$ and 0.2, in Fig. 3. Again particles are initially started in orbits with zero free eccentricity. Comparing with Fig. 3, we see no significant difference in the particle lifetimes at the two planet eccentricities. Particles placed into the chaotic zone at zero free eccentricity, would have a similar resident lifetime to those placed at zero eccentricity near a planet of zero eccentricity.

For orbits with eccentricity equal to the forced eccentricity, we find that there is a long-lived or stable region in close proximity to eccentric planets. Inside this region, particles are pumped to high eccentricity and scattered by the planet on a time-scale orders of magnitude faster than that outside this region. We have found that the width of this chaotic zone in semimajor axis is independent of the planet eccentricity. The eccentricity dispersion in the disc edge and the lifetime of particles within the zone are also nearly independent of planet eccentricity. These results suggest that there is a similarity in the dynamics of particles at zero free eccentricity and those at zero eccentricity near a planet in a circular orbit. In the following section, we explore a Hamiltonian formulation that shows that this is in fact the case.

3 HAMILTONIAN FORMULATION

In this section, we reconsider the theory of mean motion resonance overlap. We consider the role of first-order secular perturbations from the planet and the two angular perturbations that are associated with each first-order mean motion resonance. We follow the notation by Quillen (2006a). We employ the Poincaré coordinates

$$\lambda = M + \varpi, \qquad \gamma = -\varpi$$

and their associated momenta

$$L = \sqrt{GM_* a}, \qquad \Gamma = \sqrt{GM_* a}(1 - \sqrt{1 - e^2}),$$

where M_* is the mass of the star, λ is the mean longitude, M is the mean anomaly, ϖ is the longitude of pericentre, a is the semimajor axis, and e is the eccentricity. These variables are those describing the orbit of a particle or planetesimal in a plane. The Hamiltonian for the Keplerian system in these coordinates restricted to a plane is

$$H(L, \lambda; \Gamma, \gamma) = -\frac{GM_*}{2L^2} - R,$$

where R is the disturbing function, proportional to the planet mass, that depends on the coordinates of the particle and on the coordinates of the planet. The planet's semimajor axis and mass are denoted by a_p and m_p, respectively. The planet's other coordinates are subscripted in the same way. The mean motion of the particle $n = \dot{\lambda}$, where $\dot{\lambda}$ is the derivative with respect to time of λ.

Hereafter, we adopt a unit convention with distances in units of the planet's semimajor axis, a_p. Time is put in units of $\sqrt{a_p^3/GM_*}$. We define μ to be the mass ratio $\mu \equiv m_p/M_*$. At low eccentricity, $\Gamma/L \approx e^2/2$, relating the momentum Γ to the particle eccentricity. We often give the particle semimajor axis in terms of the variable $\alpha \equiv a_p/a$ if $a > a_p$ (external to the planet) and $\alpha \equiv a/a_p$ for $a < a_p$ (internal to the planet).

The unperturbed Hamiltonian or that lacking the disturbing function is

$$H_0(L, \lambda; \Gamma, \gamma) = -\frac{1}{2L^2}.$$

We consider the $j : j - k$ exterior mean motion resonance (planet is an interior perturber). We perform a canonical transformation using the mixed variable generating function

$$F_2 = I[j\lambda - (j - k)\lambda_p],$$

where $\lambda_p = n_p\, t$, leading to new variables[1]

$$I = L/j, \qquad \psi = j\lambda - (j-k)\lambda_p$$

and new Hamiltonian

$$H_0'(I, \psi; \Gamma, \gamma) = \frac{-1}{2j^2 I^2} - (j-k) I n_p.$$

We now expand around a particular value for I. Let

$$\Lambda \equiv I - I_0. \tag{2}$$

In terms of the particles' mean motion, $I_0 = n^{-1/3}/j$. Since we have adopted units $n_p = 1$, we find $I_0 = \alpha^{-1/2}/j$, where $\alpha = a_p/a$. Our Hamiltonian now reads

$$K_0(\Lambda, \psi; \Gamma, \gamma) = \text{constant} + [jn - (j-k)n_p]\Lambda - \frac{3\Lambda^2}{2j^2 I_0^4}.$$

We can write the unperturbed Hamiltonian as

$$K_0(\Lambda, \psi; \Gamma, \gamma) = a'\Lambda^2 + b'\Lambda + \text{constant},$$

with coefficients

$$\begin{aligned} a' &= -\tfrac{3}{2} j^2 \alpha^2, \\ b' &= nj - (j-k)n_p = \alpha^{3/2} j - (j-k)n_p, \end{aligned} \tag{3}$$

similar to equation (2) by Quillen (2006a). Exactly on resonance $\alpha = \left(\frac{j-k}{j}\right)^{2/3}$ and $b' = 0$. The primes here are given to differentiate a' from the semimajor axis a.

We now recover the disturbing function that is traditionally expanded as a cosine series of angles in orders of planet and particle eccentricities. We keep the terms inducing precession of the longitude of periapse and first-order (in eccentricity) or $k = 1$ terms containing ψ and ϖ. The full Hamiltonian

$$\begin{aligned} K(\Lambda, \psi; \Gamma, \gamma) = a'\Lambda^2 + b'\Lambda + c'\Gamma \\ + d'\Gamma^{1/2}\Gamma_p^{1/2}\cos(\varpi - \varpi_p) \\ + g_0\Gamma^{1/2}\cos(\psi - \varpi) \\ + g_1\Gamma_p^{1/2}\cos(\psi - \varpi_p), \end{aligned} \tag{4}$$

where $\Gamma_p \equiv (e_p^2\, L)/2$ and with the following coefficients:[2]

$$\begin{aligned} c' &= -\frac{\mu}{4}\alpha^{5/2} b^1_{3/2}, \\ d' &= \frac{\mu}{2}\alpha^{5/2} b^2_{3/2}, \\ g_0 &= -\mu\sqrt{2}\alpha^{5/4} f_{31}, \\ g_1 &= -\mu\sqrt{2}\alpha^{5/4} f_{27}. \end{aligned} \tag{5}$$

The coefficients f_{31} and f_{27} are given in table B7 by Murray & Dermott (1999). The functions $b^1_{3/2}$ and $b^2_{3/2}$ are Laplace coefficients and are functions of α. The approximate asymptotic limits for large j and $\alpha \to 1$ are $f_{31} \to j$ and $f_{27} \to -j$. We have used the approximation $e^2 \sim 2\Gamma\alpha^{1/2}$. The term proportional to $\cos(\psi - \varpi)$ is often called the e-resonance since $\Gamma^{1/2} \propto e$. The other term can be called an e'-resonance or a corotation resonance since it does not depend on the particle's longitude of perihelion or ϖ.

We first consider secular perturbations only, ignoring the g_0 and g_1 terms and considering the following:

$$K(\Gamma, \gamma) = c'\Gamma + \mathrm{d}'\Gamma^{1/2}\Gamma_p^{1/2}\cos(\varpi - \varpi_p). \tag{6}$$

We find a fixed point at

$$\begin{aligned} -\gamma &= \varpi = \varpi_p, \\ \Gamma_f^{1/2} &= \frac{b^2_{3/2}}{b^1_{3/2}}\Gamma_p^{1/2}, \end{aligned} \tag{7}$$

where $\Gamma_f \approx e^2_{\text{forced}}\, L/2$. This fixed point is equivalent to a closed orbit with eccentricity equal to the forced eccentricity

$$e_{\text{forced}} = \frac{b^2_{3/2}}{b^1_{3/2}} e_p$$

and zero free eccentricity. The coefficient c' sets the secular precession rate.

We can perform canonical transformations to new variables

$$\begin{aligned} x &= \sqrt{2\Gamma}\cos\varpi - \sqrt{2\Gamma_f}\cos\varpi_p, \\ y &= \sqrt{2\Gamma}\sin\varpi - \sqrt{2\Gamma_f}\sin\varpi_p, \\ I &= \frac{x^2 + y^2}{2}, \\ \theta &= \tan^{-1}\left(\frac{y}{x}\right). \end{aligned} \tag{8}$$

These variables were also used by Murray & Holman (1997). Here, the momentum variable I is related to the particle's free or proper eccentricity rather than the particle's eccentricity.

Recovering the Hamiltonian (equation 4) in the new variables

$$\begin{aligned} K(\Lambda, \psi; I, \theta) = a'\Lambda^2 + b'\Lambda + c'I \\ + \text{constant} \\ + g_0 I^{1/2}\cos(\psi - \theta) \\ + (g_0\Gamma_f^{1/2} + g_1\Gamma_p^{1/2})\cos(\psi - \varpi_p). \end{aligned} \tag{9}$$

The expansion about the fixed point associated with the forced eccentricity does not change the form of the term normally associated with the first-order mean motion resonance, that is proportional to $\cos(\psi - \theta)$. Consequently, the resonance libration time and width are unchanged. The predicted semimajor axis where resonance overlap occurs based on these resonance widths would be identical to that for a planet in a circular orbit (see below).

However, the width of the corotation resonance differs from that predicted using equation (4). The coefficient describing the strength of this resonance [$\propto \cos(\psi - \varpi_p)$ in equation 9], can be rewritten as

$$\mu\sqrt{2}\alpha^{5/4}(f_{31}e_{\text{forced}} + f_{27}e_p)\cos(\psi - \varpi_p),$$

using the coefficients listed in equations (5). Since f_{27} and f_{31} have opposite signs, the forced eccentricity term will tend to cancel the other term. In the high j limit, the forced eccentricity equals the planet's eccentricity and $f_{27} \approx -f_{31}$ so these two terms cancel. The $\mu^{2/7}$ law is only valid for the high j limit. Consequently, the corotation resonance completely cancels near the planet for orbits with zero free eccentricity. This implies that the dynamics of particles at low eccentricity near a planet in a circular orbit is similar to the dynamics of particles at low free eccentricity near a planet in an eccentric orbit.

We note that our expansion above is valid only to first order in the particle and planet eccentricity. At high particle and planet eccentricity, additional resonance terms become important, and the low eccentricity expansion is no longer valid. The above Hamiltonian (equation 9) is not restricted to zero free eccentricity but to low values of the free eccentricity due to the low degree of the expansion.

[1] There is an error in the I variable definition by Quillen (2006a).

[2] Equation (4) by Quillen (2006a) for c should have had a factor of $\alpha^{3/2}$.

3.1 Rederiving the 2/7th law and the eccentricity dispersion in the disc edge

In Section 2, we numerically measured the eccentricity dispersion in the disc edge, finding that it too does not significantly depend on planet eccentricity. Outside the chaos zone, planetesimals still experience perturbations from the planet. These perturbations have a characteristic size set by size of perturbations in the nearest mean motion resonance that is not wide enough to overlap others and so is not part of the chaotic zone. Since particles in the edge reside outside the chaotic zone, the velocity dispersion does not increase with time. In this section, we check that our formulation can correctly predict the location of resonance overlap. We then predict eccentricity variations that would be predicted by considering the role of the last resonance that is not part of the chaotic zone.

The width of the resonance can be thought of as the range of semimajor axis over which the resonance has a large effect. To estimate the first-order resonance width, we rescale the momentum and put the Hamiltonian in a unitless form (e.g. as done by Murray & Dermott 1999 in section 8.8 or by Quillen 2006a in section 3). The factors used to rescale the Hamiltonian set the resonance width. We perform a canonical transformation of the Hamiltonian given in equation (9) lacking the corotation term or

$$K(\Lambda, \psi; I, \theta) = a'\Lambda^2 + b'\Lambda + c'I + g_0 I^{1/2}\cos(\psi - \theta)$$

with generating function

$$F_2 = J_1(\theta - \psi) + J_2\psi$$

leading to new variables

$$\begin{aligned} J_2 - J_1 &= \Lambda, \qquad \phi = \theta - \psi \\ J_1 &= I, \qquad \psi = \psi \end{aligned} \tag{10}$$

and new Hamiltonian

$$K'(I, \phi; J_2, \psi) = a'\left(I^2 + J_2^2\right) + \left(c' - 2a'J_2 - b'\right)I + b'J_2 + g_0 I^{1/2}\cos\phi. \tag{11}$$

Note that J_2 is conserved and is small for initial conditions near resonance with small initial free eccentricity (or I). Dropping constant terms and setting

$$B = c' - 2a'J_2 - b', \tag{12}$$

the Hamiltonian in equation (12) becomes

$$K'(I, \phi) = a'I^2 + BI + g_0 I^{k/2}\cos\phi.$$

Here, the coefficient B determines the distance from resonance. By rescaling momentum and time

$$\begin{aligned} \bar{I} &= \left|\frac{g_0}{a'}\right|^{-2/3} I, \\ \tau &= |g_0|^{2/3}\,|a'|^{1/3}\,t, \end{aligned} \tag{13}$$

we can write this as

$$\bar{K}(\bar{I}, \phi) = \bar{I}^2 + \bar{b}\bar{I} - \bar{I}^{1/2}\cos\phi, \tag{14}$$

where

$$\bar{b} = B|g_0|^{-2/3}\left|a'\right|^{-1/3} \tag{15}$$

sets the distance from exactly on resonance. The resonance is only strong over a range $\Delta\bar{b} \sim 1$ (e.g. see fig. 8.10 by Murray & Dermott 1999) corresponding to a range of particle mean motions. Assuming slow secular precession and neglecting the term $\propto J_2$, the variation $\Delta B \sim -\Delta b'$ (equation 13). Equation (3) allows us to relate $\Delta b'$ to the range of mean motions over which the resonance is strong $\Delta b' \sim j\Delta n$. Equation (16) then implies that the resonance is strong over a range of mean motions of size

$$\Delta n \sim j^{-1}\,|g_0|^{2/3}\left|a'\right|^{1/3}.$$

For resonances near the planet, we can use the asymptotic limit ($\alpha \to 1, j$ large) that gives $g_0 \to \mu j$. Subbing in for g_0 and considering the range of semimajor axis rather than mean motion, the resonance width is

$$\Delta a \sim \mu^{2/3} j^{1/3},$$

where we have used $\Delta n \sim 3/2\Delta a$. Using a spacing between $j : j - 1$ resonances of $\Delta a \sim (2/3)\, j^{-2}$, we find that the resonances overlap at the resonance with

$$j \sim \mu^{-2/7}.$$

The semimajor axis corresponding to the $j : j - 1$ resonance at the chaotic zone boundary is set by the above j. The $j : j - 1$ mean motion resonance located at a semimajor axis of $a = (1 - 1/j)^{-2/3} \sim 1 + 2/(3j)$ for large j. The distance between the planet and chaotic zone boundary, δa_z, in semimajor axis, that is, chaotic zone width, is then

$$\delta a_z \sim \mu^{2/7}, \tag{16}$$

recovering the 2/7th law (Wisdom 1980; Duncan et al. 1989; Murray & Holman 1997; Mudryk & Wu 2006).

The eccentricity change or libration width in the resonance just outside the boundary would have size

$$I \sim \left|\frac{g_0}{a'}\right|^{2/3}, \tag{17}$$

where we have used the libration width (given by the scaling factor for $\bar{I}$ in equation 14) or

$$I \sim \mu^{2/3} j^{-2/3}. \tag{18}$$

Subbing in $j \sim \mu^{-2/7}$ at the chaotic zone boundary gives $I \sim \mu^{6/7}$ and an eccentricity dispersion of

$$u_e \sim \mu^{3/7} \tag{19}$$

just outside the chaos zone. This dispersion could set the slope of the density distribution in the disc edge (e.g. Quillen 2006b). The scaling predicted by equation (19) is shown compared to numerical measurements of the eccentricity dispersion in the disc edge in Fig. 2. It provides a good fit to the measurements and is independent of planet eccentricity as predicted by considering equation (9) for orbits with low free eccentricity.

4 SUMMARY AND DISCUSSION

In this paper, we have investigated the dynamics of low free eccentricity collisionless massless particles in the plane near a planet on a eccentric orbit. By determining the semimajor axis at which the particle lifetime increases, we measure the width of the chaotic zone near the planet. For eccentricity $e_p < 0.3$, we find that the chaotic zone width is independent of the planet's eccentricity and matches that predicted by the 2/7th law. The eccentricity dispersion in the disc edge and the lifetime of particles within the chaotic zone are also nearly independent of planet eccentricity. These results suggest that there is a similarity in the dynamics of particles at zero free eccentricity and those at zero eccentricity near a planet in a circular orbit.

To account for our numerical results, we have explored the dynamics of a Hamiltonian system that takes into account first-order secular perturbations and the two terms that comprise each first-order mean motion resonance. With a coordinate transformation, we have rewritten the Hamiltonian in terms of an action variable that depends on the free eccentricity rather than the eccentricity. At low free eccentricity, we find that the new Hamiltonian resembles the Hamiltonian of a low-eccentricity particle near a planet in a circular orbit. This accounts for the lack of sensitivity of the particle dynamics on planet eccentricity.

For orbits with eccentricity equal to the forced eccentricity, there is a region in the plane with longer-lived orbits (compared to the planet orbital period) in close proximity to eccentric planets. Three-dimensional simulations that incorporate collisions are needed to see if these orbits tend to be populated by long-lived particles, as proposed for Fomalhaut's eccentric ring (Quillen 2006b).

ACKNOWLEDGMENTS

We thank the referee, Dr Tsiganis, for numerous comments that have significantly improved this manuscript. Support for this work was in part provided by National Science Foundation grants AST-0406823 and PHY-0552695 the National Aeronautics and Space Administration under Grant No. NNG04GM12G issued through the Origins of Solar Systems Program, and HST-AR-10972 to the Space Telescope Science Institute.

REFERENCES

Aumann H. H., 1985, PASP 97, 885
Barnes R., Raymond S. N., 2004, ApJ, 617, 569
Dent W. R. F., Walker H. J., Holland W. S., Greaves J. S., 2000, MNRAS, 314, 702
Duncan M., Quinn T., Tremaine S., 1989, Icarus, 82, 402
Gillett F., 1985, in Israel F. P., ed., Light on Dark Matter. D. Reidel Co., Dordrecht, p. 61
Holland W. S. et al., 1998, Nat, 392, 788
Holland W. S. et al., 2003, ApJ, 582, 1141
Holman M. J., Wisdom J., 1993, AJ, 105, 1987
Holman M. J., Wiegert P. A., 1999, AJ, 117, 621
Kalas P., Graham J. R., Clampin M., 2005, Nat, 435, 1067
Lecar M., Franklin F., Murison M., 1992, AJ, 104, 1230
Lecar M., Franklin F. A., Holman M. J., Murray N. J., 2001, ARA&A, 39, 581
Lepage I., Duncan M. J., 2004, AJ, 127, 1755
Marsh K. A., Velusamy T., Dowell C. D., Grogan K., Beichman C. A., 2005, ApJ, 620, L47
Mudryk L. R., Wu Y., 2006, ApJ, 639, 423
Murray C. D., Dermott S. F., 1999, Solar System Dynamics. Cambridge Univ. Press, Cambridge
Murray N., Holman M., 1997, AJ, 114, 1246
Quillen A. C., 2006a, MNRAS, 372, L14
Quillen A. C., 2006b, MNRAS, 365, 1367
Rasio F. A., Ford E. B., 1996, Sci, 274, 954
Stapelfeldt K. R. et al., 2004, ApJS, 154, 458
Tsiganis K., Gomes R., Morbidelli A., Levison H. F., 2005, Nat, 435, 7041, 459
Winter O. C., Murray C. D., 1997, A&A, 319, 290
Wisdom J., 1980, AJ, 85, 1122
Wisdom J., 1985, Icarus, 63, 272

This paper has been typeset from a TEX/LATEX file prepared by the author.